Pingfeng Wang
Assistant Professor
Mem. ASME,
Department of Industrial and
Manufacturing Engineering,
Wichita State University,
Wichita, KS 67226
e-mail: pingfeng.wang@wichita.edu

Chao Hu
Graduate Student
Department of Mechanical Engineering,
University of Maryland at College Park,
College Park, MD 20742
e-mail: huchaost@umd.edu

Byeng D. Youn[1]
Assistant Professor
Mem. ASME,
School of Mechanical and
Aerospace Engineering,
Seoul National University,
Seoul 151-742, South Korea
e-mail: bdyoun@snu.ac.kr

A Generalized Complementary Intersection Method (GCIM) for System Reliability Analysis

This paper presents a Generalized Complementary Intersection Method (GCIM) that can predict system reliability for series, parallel, and mixed systems. The GCIM is an extension of the original study, referred to as the Complementary Intersection Method (CIM). The CIM was developed to assess system reliability for series systems. The contribution of this paper is to generalize the original CIM so that it can be used for system reliability analysis regardless of system structures (series, parallel, and mixed system). First, we derive a closed-form system reliability formula for a parallel system through its transformation into a series system using De Morgan's law. Second, a unified system reliability analysis framework is proposed for mixed systems by defining a new System Structure matrix (SS-matrix) and employing the Binary Decision Diagram (BDD) technique. The SS-matrix is used to present any system structure in a comprehensive matrix form. Then the BDD technique together with the SS-matrix automates the process to identify system's mutually exclusive path sets, of which each path set is a series system. As a result, system reliability with any system structure can be decomposed into the probabilities of the mutually exclusive path sets. Five engineering examples are used to demonstrate that the proposed GCIM can assess system reliability regardless of the system structures.
[DOI: 10.1115/1.4004198]

1 Introduction

Considerable advances have been made in the field of reliability analysis [1–4] and Reliability-Based Design Optimization (RBDO) [5–9] for engineered system analysis and design under uncertainty. In order to ensure high reliability of complex engineered systems against deterioration or natural and man-made hazards, it is essential to have an efficient and accurate method for estimating the probability of system failure regardless of different system configurations. Although tremendous advances have been made in component reliability analysis and design optimization, the research in system reliability analysis has been stagnant due to the complicated nature of the multiple system failure modes and their interactions, as well as the costly computational expense of system reliability evaluation. Since system reliability prediction is of great importance in civil, aerospace, mechanical, and electrical engineering fields, its technical development will have an immediate and major impact on engineered system designs.

Due to the difficulties, most system reliability analysis methods provide the bounds of system reliability. Ditlevsen and Bjerager proposed the most widely used second-order system reliability bounds method, which gives much tighter bounds compared with the first-order bounds for both series and parallel systems [10]. Other equivalent forms of the bounds of Ditlevsen and Bjerager were given by Thoft-Christensen and Murotsu [11], Karamchandani [12], Xiao and Mahadevan [13], and Ramachandran [14]. Song and Der Kiureghian formulated system reliability to a Linear Programming (LP) problem, referred to as the LP bounds method [15] and latterly the matrix-based system reliability method [16]. The LP bounds method is able to calculate the optimal bounds for system reliability based on available reliability information. However, it is extremely sensitive to accuracy of the available reliability information, which is the probabilities for the first-, second-, or higher-order joint safety events. To assure high accuracy of the LP bounds method for system reliability prediction, the probabilities must be given very accurately. Besides the system reliability bound methods, one of the most popular approaches is the multimodal Adaptive Importance Sampling method, which is found satisfactory for the system reliability analysis of large structures [17,18]. The integration of surrogate model techniques with Monte Carlo Simulation (MCS) can be an alternative approach to system reliability prediction as well [19]. This approach, which can construct the surrogate models for multiple limit-state functions to represent a joint failure region, is quite practical but accuracy of the approach depends on fidelity of the surrogate models. It is normally expensive to build accurate surrogate models. Most recently, Youn and Wang [20] introduced a novel concept of the complementary intersection event and proposed the Complementary Intersection Method (CIM) for series system reliability analysis. The CIM provides not only a unique formula for system reliability but also an effective numerical method to evaluate the system reliability with high efficiency and accuracy. The CIM decomposes the probabilities of high-order joint failure events into probabilities of complementary intersection events. For large scale systems, a CI-matrix was proposed to store the probabilities of component safety and complementary intersection events. Then, series system reliability can be efficiently evaluated by advanced reliability methods, such as dimension reduction method and stochastic collocation method. However, the application of the CIM has been limited to a series system only.

This paper presents a Generalized CIM (GCIM) framework, which enables the use of the original CIM for system reliability analysis with any system structures (series, parallel, and mixed systems). The SS-matrix is proposed to characterize any system structure in a comprehensive manner and the Binary Decision Diagram (BDD) technique is employed to identify system's mutually exclusive path sets using the SS-matrix, of which each path set is a series system. As a result, system reliability with any system structure can be decomposed into the probabilities of the mutually exclusive path sets, which can be evaluated using various numerical methods for reliability analysis. Five examples are

[1]Corresponding author.

Contributed by the Design Automation Committee of ASME for publication in the JOURNAL OF MECHANICAL DESIGN. Manuscript received February 28, 2011; final manuscript received May 3, 2011; published online July 7, 2011. Assoc. Editor: Zissimos P. Mourelatos.

used to demonstrate that the proposed GCIM can assess system reliability regardless of the system structures. Section 2 reviews the CIM and CI-matrix. Section 3 presents the GCIM for system reliability analysis for series, parallel, and mixed systems. The proposed method is demonstrated with five case studies in Sec. 4. Section 5 concludes this paper.

2 Complementary Intersection Method (CIM)

This section reviews the Complementary Intersection Method (CIM) [20].

2.1 CI Event and Probability Decomposition Theorem. Here we review the definition of CI event and the probability decomposition theorem.

Definition. *Complementary Intersection (CI) Event*: *Let an Nth-order CI event denote* $E_{12,\ldots,N} \equiv \{X|G_1G_2\cdots G_N \le 0\}$, *where the component safety (or first-order CI) event is defined as* $E_i = \{X|G_i \le 0,\ i = 1, 2,\ldots,N\}$. *The defined Nth-order CI event is actually composed of N distinct intersections of component events* E_i *and their complements* $\bar{E}_j$ *in total where* $i, j = 1,\ldots, N$ *and* $i \neq j$. *For example, for the second-order CI event* E_{ij}, *it is composed of two distinct intersection events,* $E_1\bar{E}_2$ and $\bar{E}_1E_2$. *These two events are the intersections of* E_1 (or E_2) *and the complementary event of* E_2 (*or* E_1).

THEOREM. *Decomposition of the Probability of an Nth-Order Joint Safety Event. With the definition of the CI event, the probability of an Nth-order joint safety event can be decomposed into the probabilities of the component safety events and the CI events as*

$$P\left(\bigcap_{i=1}^{N} E_i\right) = \frac{1}{2^{N-1}}\left[\sum_{i=1}^{N} P(E_i) - \sum_{\substack{i=1;\\ j=2;\\ i<j}}^{N} P(E_{ij}) + \sum_{\substack{i=1;\\ j=2;\\ k=3\\ i<j<k}}^{N} P(E_{ijk}) + \cdots + (-1)^{m-1} \sum_{\substack{i=1;\\ j=2;\\ \vdots\\ l=m\\ i<j<\cdots<l}}^{N} P\left(\underbrace{E_{ij\cdots l}}_{m}\right) + \cdots + (-1)^{N-1} P(E_{12\cdots N})\right] \tag{1}$$

The detailed derivation of Eq. (1) can be found in Ref. [20]. It is noted that each CI event has its own limit state function, which enables the use of any reliability analysis methods. In general, higher-order CI events are expected to be highly nonlinear. Considering the tradeoff between computational efficiency and accuracy, this paper uses the probabilities of the first- and second-order CI events in Eq. (1) for system reliability analysis. However, more terms in Eq. (1) can be employed as advanced reliability analysis methods are developed in the future.

Based on the definition of the CI event, the second-order CI event can be denoted as $E_{ij} \equiv \{X \mid G_iG_j \le 0\}$. The CI event can be further expressed as $E_{ij} = \bar{E}_iE_j \cup E_i\bar{E}_j$ where the component failure events are defined as $\bar{E}_i = \{X \mid G_i > 0\}$, $\bar{E}_j = \{X \mid G_j > 0\}$. The CI event E_{ij} is thus composed of two events: $E_i\bar{E}_j = \{X \mid G_i \le 0 \cap G_j > 0\}$ and $\bar{E}_iE_j = \{X \mid G_i > 0 \cap G_j \le 0\}$. Since the events, $\bar{E}_iE_j$ and $E_i\bar{E}_j$, are disjoint, the probability of the CI event E_{ij} can be expressed as

$$\begin{aligned} P(E_{ij}) &\equiv P(X|G_iG_j \le 0) \\ &= P(X|G_i > 0 \cap G_j \le 0) + P(X|G_i \le 0 \cap G_j > 0) \\ &= P(\bar{E}_iE_j) + P(E_i\bar{E}_j) \end{aligned} \tag{2}$$

Based on the probability theory, the probability of the second-order joint safety event $E_i \cap E_j$ can be expressed as

$$\begin{aligned} P(E_iE_j) &= P(E_i) - P(E_i\bar{E}_j) \\ &= P(E_j) - P(\bar{E}_iE_j) \end{aligned} \tag{3}$$

From Eqs. (2) and (3), the probabilities of the second-order joint safety and failure events can be decomposed as

$$P(E_iE_j) = \frac{1}{2}\left[P(E_i) + P(E_j) - P(E_{ij})\right] \tag{4}$$

$$P(\bar{E}_i\bar{E}_j) = 1 - \frac{1}{2}\left[P(E_i) + P(E_j) + P(E_{ij})\right] \tag{5}$$

2.2 CI-Matrix. For large-scale systems, the CI events can be conveniently written in the CI-matrix. For instance, if the system includes m components in total, the CI-matrix is defined as

$$\text{CI} = \begin{bmatrix} P(E_1) & P(E_{12}) & P(E_{13}) & \cdots & P(E_{1m}) \\ - & P(E_2) & P(E_{23}) & \cdots & P(E_{2m}) \\ - & - & P(E_3) & \cdots & P(E_{3m}) \\ - & - & - & \ddots & \vdots \\ - & - & - & - & P(E_m) \end{bmatrix} \tag{6}$$

In the upper triangular CI-matrix, the diagonal elements correspond to the component reliabilities (or probabilities of the first-order CI events) and the element on the ith row and jth column corresponds to the probability of the second-order CI event E_{ij} if $j < i$. The probabilities of the second-order joint safety and failure events in Eqs. (4) and (5) can be evaluated with the probabilities of all component safety and complementary intersection events found from the CI-matrix. The CI-matrix thus facilitates the evaluation of system reliability. The probability of the complementary intersection events can be computed using any reliability analysis method, such as the MCS, First-Order Reliability Method (FORM), Second-Order Reliability Method (SORM), Eigenvector Dimension Reduction (EDR) method, Stochastic Expansion (SE) methods, and so on.

3 Generalized Complementary Intersection Method for System Reliability Analysis

Here we attempt to generalize the original CIM for system reliability analysis with any system structure (series, parallel, and

mixed systems). Section 3.1 will briefly review the CIM for series system reliability analysis from Ref. [20]. The proposed GCIM for parallel and mixed system reliability analysis are developed in Secs. 3.2 and 3.3, respectively. Section 3.4 provides the GCIM framework for system reliability analysis.

3.1 System Reliability Analysis for Series Systems. Although the second-order system reliability bounds method or the LP bounds method can generally give fairly narrow system reliability bounds, they cannot provide system reliability uniquely. The authors proposed the explicit formula for series system reliability assessment. This original CIM can provide an alternative way of assessing system reliability.

Considering a structural serial system with m components, the probability of system failure can be expressed as

$$P_{fs} = P\left(\bigcup_{i=1}^{m} \bar{E}_i\right) \tag{7}$$

where P_{fs} represents the probability of system failure and $\bar{E}_i$ denotes the failure event of the ith component. Based on the well-known Boolean bounds in Eq. (8), the first-order system reliability bound is given in Eq. (9),

$$\max_i(P(\overline{E}_i)) \le P\left(\bigcup_{i=1}^{m} \bar{E}_i\right) \le \sum_{i=1}^{m} P(\overline{E}_i) \tag{8}$$

$$\max\left[P(\overline{E}_i)\right] \le P_{fs} \le \min\left[\sum_{i=1}^{m} P(\overline{E}_i), 1\right] \tag{9}$$

However, these methods provide wide bounds of system reliability. Thus, the second-order bounds method proposed by Ditlevsen and Bjerager [21] in Eq. (10) is widely used because it gives quite narrow bounds of system reliability,

$$P(\overline{E_1}) + \sum_{i=2}^{m} \max\left\{\left[P(\overline{E}_i) - \sum_{j=1}^{i-1} P(\overline{E_iE_j})\right], 0\right\} \le P_{fs} \le \min\left\{\left[\sum_{i=1}^{m} P(\overline{E}_i) - \sum_{i=2}^{m} \max_{j<i} P(\overline{E_iE_j})\right], 1\right\} \tag{10}$$

where E_1 is the event having the largest probability of failure.

Since the probabilities of all events are non-negative, the following inequalities must be satisfied as

$$\max_i(P(\overline{E}_i)) \le \sqrt{\sum_{i=1}^{m} \left[P(\overline{E}_i)\right]^2} \le \sum_{i=1}^{m} P(\overline{E}_i) \tag{11}$$

Based on Eqs. (10) and (11), the probability of system failure (P_{fs}) of a serial system failure can be simplified to a unique explicit formula as

$$P_{fs} \cong P(\overline{E_1}) + \sum_{i=2}^{m} \left\langle P(\overline{E}_i) - \sqrt{\sum_{j=1}^{i-1} \left[P(\overline{E_iE_j})\right]^2} \right\rangle \tag{12}$$

It is proven in Ref. [20] that this approximate probability lies in the second-order bounds in Eq. (10). From Eq. (12), serial system reliability can be assessed as (1-the probability of system failure) and formulated as

$$R_{s\_\text{series}} = P(E_1E_2\cdots E_{m-1}E_m) \cong P(E_1) - \sum_{i=2}^{m} \left\langle P(\overline{E}_i) - \sqrt{\sum_{j=1}^{i-1} \left[P(\overline{E_iE_j})\right]^2} \right\rangle$$
$$\text{where } \langle A\rangle \equiv \begin{cases} A & \text{if } A > 0 \\ 0 & \text{if } A \le 0 \end{cases} \tag{13}$$

Note that the terms inside the brackets, $\langle\bullet\rangle$, should be ignored if they are less than zero and R_s should be set to zero if the approximated one given by Eq. (13) is less than zero. Equation (13) provides an explicit and unique formula for system reliability assessment based on the second-order reliability bounds shown in Eq. (10) and an inequality Eq. (11). The CI-matrix facilitates the evaluation of system reliability for large-scale systems with multiple failure events. The probability of the CI events can be computed using any reliability analysis method, such as MCS, FORM, SORM, EDR method, or SE methods.

3.2 System Reliability Analysis for Parallel Systems. A parallel system reliability formula can be obtained based on the formula of series system reliability by using De Morgan's law. According to De Morgan's law, the probability of parallel system failure can be expressed as

$$P\left(\bigcap_{i=1}^{m} \bar{E}_i\right) = 1 - P\left(\overline{\bigcap_{i=1}^{m} \bar{E}_i}\right) = 1 - P\left(\bigcup_{i=1}^{m} E_i\right) \tag{14}$$

where E_i is the ith component failure event.

Equation (14) relates the probability of parallel system failure with the probability of series system safety (reliability). If we treat E_i as the ith component failure event in a series system, the right-hand side of Eq. (14) is then the series system reliability. Based on this relationship, the probability of parallel system failure can be obtained from Eq. (13) by treating the safe events in the series system as the failure events in the parallel system as

$$P\ (\text{failure of a parallel system}) \cong P(\overline{E_1}) - \sum_{i=2}^{m} \left\langle P(E_i) - \sqrt{\sum_{j=1}^{i-1} \left[P(E_iE_j)\right]^2} \right\rangle$$
$$\langle A\rangle \equiv \begin{cases} A & \text{if } A > 0 \\ 0 & \text{if } A \le 0 \end{cases} \tag{15}$$

Finally, parallel system reliability can be obtained from Eq. (15) by one minus the probability of system failure as

$$R_{s\_\text{parallel}} \cong P(E_1) + \sum_{i=2}^{m} \left\langle P(E_i) - \sqrt{\sum_{j=1}^{i-1} \left[P(E_iE_j)\right]^2} \right\rangle$$
$$\langle A\rangle \equiv \begin{cases} A & \text{if } A > 0 \\ 0 & \text{if } A \le 0 \end{cases} \tag{16}$$

3.3 Mixed System Reliability Analysis. A mixed system may have various system structures. There is no unique system reliability formula available for a mixed system. This study develops a generic procedure for mixed system reliability analysis with an aim to produce a unique system reliability formula. The developed procedure is introduced in the following with an arbitrary mixed system structure. Considering a mixed system with N components, the following procedure can be proceeded to carry out system reliability analysis.

Step I—Constructing a System Structure Matrix. An SS-matrix, a 3-by-M, is proposed in this study to characterize any system structural configuration (components and their connections) in a

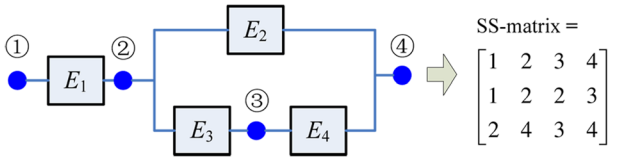

Fig. 1 Example to show the conversion of a system block diagram to SS-matrix

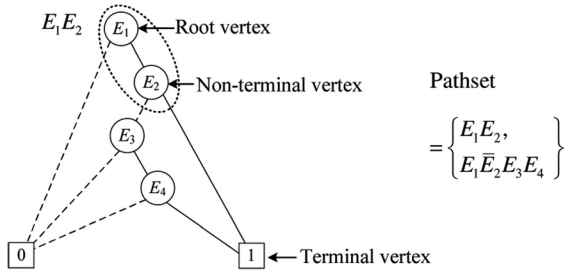

Fig. 2 BDD diagram and the mutually exclusive path sets

matrix form. The SS-matrix contains the information about the constituting components and their connection. The first row of the matrix contains component numbers, while the second and third rows correspond to the starting and end nodes of the components. Generally, the total number of columns of an SS-matrix, M, is equal to the total number of system components, N. In the case of complicated system structures, one component may repeatedly appear in between different sets of nodes and, consequently, M could be larger than N, e.g., a 2-out-of-3 system.

Let us consider an example of a mixed system consisting of four components, as shown in Fig. 1. The SS-matrix for the system can be constructed as a 3×4 matrix, as shown in Fig. 1. The first column of the system structure matrix, $[1,1,2]^T$, indicates that the first component connects nodes 1 and 2.

Step II—Finding Mutually Exclusive System Path Sets. Based on the SS-matrix, the Binary Decision Diagram (BDD) technique [22,23] can be employed to find the mutually exclusive system path sets, of which each path set is a series system. In probability theory, two events are said to be mutually exclusive if they cannot occur at the same time or, in other words, the occurrence of any one of them automatically implies the nonoccurrence of the other. Here, system path sets are said to be mutually exclusive if any two of them are mutually exclusive. We note that, without the SS-matrix, it is not easy for the BDD technique to automate the process to identify the mutually exclusive path sets. Detailed information regarding the fundamentals and implementation details of the BDD can be found in the Appendix. The mixed system shown in Fig. 1 can be decomposed into the two mutually exclusive path sets using the BDD, which is shown in Fig. 2. Although the path sets $E_1\bar{E}_2E_3E_4$ and $E_1E_3E_4$ represent the same path that goes through from the left terminal 1 to the right terminal 4 in Fig. 1, the former belongs to the mutually exclusive path sets in Fig. 2 while the latter does not. This is due to the fact that the path sets $E_1E_3E_4$ and E_1E_2 are not mutually exclusive. We also note, however, that we could still construct another group of mutually exclusively path sets, $\{E_1E_3E_4, E_1E_2\bar{E}_3\}$, which contains the path set $E_1E_3E_4$ as a member. This is due to the fact that a mixed system may have multiple BDDs with different configurations depending on the ordering of nodes in BDDs and these BDDs result in several groups of mutually exclusive path sets, among which the one with the smallest number of path sets is desirable. Another point deserving of notice is that the mixed system considered here consists of only two mutually exclusive path sets. In cases of more than two mutually exclusive path sets, any two path sets are mutually exclusive. This suggests that the system path sets can equivalently be said to be pairwise mutually exclusive.

Step III—Evaluating All Mutually Exclusive Path Sets and System Reliability. Due to the property of the mutual exclusiveness, the mixed system reliability, R_{s_mixed}, is the sum of the probabilities of all paths as

$$R_{s\_\text{mixed}} = P\left(\bigcup_{i=1}^{N_p} \text{Path}_i\right) = \sum_{i=1}^{N_p} P(\text{Path}_i) \tag{17}$$

where Path_i is the ith mutually exclusive path set obtained by the BDD and N_p is the total number of mutually exclusive path sets. For the system in Fig. 1, the system reliability can be calculated as

$$\begin{aligned} R_{s\_\text{mixed}} &= P\left(\bigcup_{i=1}^{2} \text{Path}_i\right) = \sum_{i=1}^{2} P(\text{Path}_i) \\ &= P(E_1E_2) + P(E_1\bar{E}_2E_3E_4) \end{aligned} \tag{18}$$

where the probability of each individual path set can be calculated using the series system reliability formula given by Eq. (13).

3.4 GCIM Framework for System Reliability Analysis. While a series system or a parallel system can be viewed as a special case of a mixed system, the proposed generalized CIM framework with the SS-matrix and BDD can perform system reliability analysis with any system structures (series, parallel, and mixed). Figure 3 shows a generalized CIM framework for system reliability. As shown in Fig. 3, the first step of the CIM framework is to prepare the system input information, such as system performances (or limit state functions), their relation (or system structure), and random input variables associated with the system. Subsequently, the GCIM requires the four-step process for the system reliability analysis, (1) constructing the SS-matrix, (2) evaluating the CI-matrix using advanced probability analysis methods as introduced in Sec. 2, (3) identifying mutually exclusive path sets using the BDD with the SS-matrix,

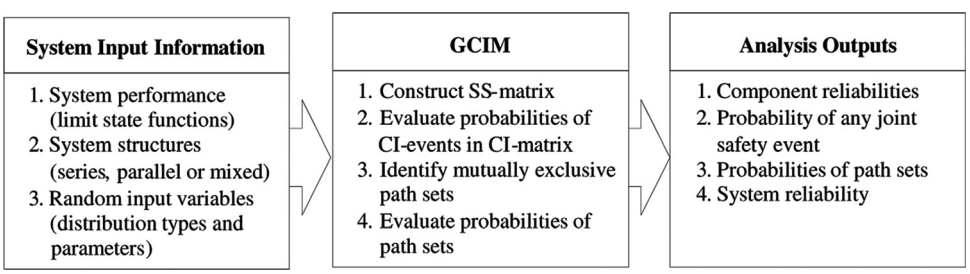

Fig. 3 GCIM framework for system reliability analysis

Table 1 Statistical information of input random variables for combustion engine

Random variable	Mean	Standard deviation	Distribution type
b (mm)	—	0.40	Normal
c_r (mm)	—	0.15	Normal
d_E (mm)	—	0.15	Normal
d_I	—	0.05	Normal
ω, ($\times 10^{-3}$)	—	0.25	Normal

and (4) evaluating the probabilities of all path sets. After completing the four-step process, the GCIM can provide various outputs, such as component reliabilities, probabilities of any joint failure event, probabilities of path sets, and the system reliability. This GCIM framework can be generic because it can assess system reliability for any system structure (series, parallel, and mixed systems) using advanced reliability methods.

4 Case Studies

In the following, we present five case studies for a series system, a parallel system, and three mixed systems, respectively, to demonstrate the efficiency and accuracy of the proposed GCIM for system reliability analysis. For each case study, the generalized CIM framework is demonstrated in a wide range of system reliability levels and compared with MCS. For series and parallel systems, the results of the generalized CIM framework are also compared with First-Order Bound (FOB) and Second-Order Bound (SOB) methods. The main objective of the case studies is to demonstrate the theoretical accuracy of the proposed generalized CIM framework for system reliability analysis. So in the five examples we focus on a mathematical error produced by a system reliability formula rather than a numerical error by a numerical method. In order to eliminate the numerical error in system reliability analysis, MCS with a large sample size was used to evaluate the CI-matrix as shown in each case study.

4.1 Example 1. An Internal Combustion Engine Series System. The following internal combustion engine case study is used to demonstrate the application of the generalized CIM for series system reliability analysis. Five random variables are considered in this example: the cylinder bore b, compression ratio c_r, exhaust valve diameter d_E, intake valve diameter d_I, and the revolutions per minute (rpm) at peak power, ω. All the random variables are assumed to follow normal distribution with statistical information shown in Table 1. More detailed information of this example can be found in Ref. [24]. From a thermodynamic viewpoint, nine component safety events are defined as follows:

Table 2 Eight different design points for system reliability analysis

Designs points	Mean values for random variables				
	b	c_r	d_E	d_I	ω
1	82.1025	35.8039	30.3274	9.3397	5.2827
2	82.3987	36.1754	30.4835	9.3684	5.5983
3	82.5511	36.3630	30.5676	9.3811	5.7550
4	82.6770	36.5187	30.6334	9.3920	5.8901
5	82.8234	36.7006	30.7121	9.4049	5.9498
6	82.8750	36.7655	30.7407	9.4096	5.9754
7	82.9204	36.8222	30.7657	9.4137	5.9772
8	82.9977	36.9197	30.8084	9.4204	5.9795

$$
\begin{aligned}
E_1 &= \{1.2N_c b - 400 \le 0\} \text{ (min. bore wall thickness)}\\
E_2 &= \left\{[8V/(200\pi N_c)]^{0.5} - b \le 0\right\} \text{ (max. engine height)}\\
E_3 &= \{d_I + d_E - 0.82b \le 0\} \text{ (valve geometry and structure)}\\
E_4 &= \{0.83d_I - d_E \le 0\} \text{ (min. value diameter ratio)}\\
E_5 &= \{d_E - 0.89d_I \le 0\} \text{ (max. value diameter ratio)}\\
E_6 &= \left\{9.428 \times 10^{-5}[4V/(\pi N_c)]\left(\omega/d_I^2\right) - 0.6C_s \le 0\right\}\\
&\quad \text{(max. Mech/Index)}\\
E_7 &= \{0.045b + c_r - 13.2 \le 0\} \text{ (knock} - \text{limit compression ratio)}\\
E_8 &= \{\omega - 6.5 \le 0\} \text{ (max. torque converter rpm)}\\
E_9 &= \left\{230.5Q\eta_{tw} - 3.6 \times 10^6 \le 0\right\} \text{ (max. fuel economy)} \qquad (19)
\end{aligned}
$$

where

$$
\eta_{tw} = 0.85951\left(1 - c_r^{-0.33}\right) - S_v, V = 1.859 \times 10^6\,\text{mm}^3
$$
$$
Q = 43,958\ \text{kJ/kg}, C_s = 0.44, \text{ and } N_c = 4
$$

In this study, system reliability analyses are performed at the eight different design points as listed in Table 2. These design points are the reliability-based optimum designs with eight different target component reliability levels from 80% to 99.9%. In the RBDO problem, the objective is to maximize the power output per unit displacement of an internal combustion engine while meeting nine specific fuel economy and packaging constraints detailed in Eq. (19). Detailed information of the objective function can be found in Ref. [24]. The results of system reliability analysis at these design points are summarized in Table 3 and also graphically shown in Fig. 4. From the results, it is found that the first-order bounds method gives too wide bounds to be of practical use. On the contrary, the second-order bounds method gives tighter bounds. It is expected based on the results that the GCIM can predict system reliabilities accurately at various reliability levels and the estimation errors tend to be lower at high system reliability

Table 3 Results of system reliability analysis with MCS, FOB using MCS, SOB using MCS, and GCIM using MCS ($N = 1 \times 10^6$)

Analysis method		System reliability level at each design							
		1	2	3	4	5	6	7	8
FOB	Upper	0.9989	0.9899	0.9745	0.9495	0.8984	0.8742	0.8490	0.7988
	Lower	0.9949	0.9506	0.8744	0.7432	0.5367	0.4318	0.3410	0.1513
SOB	Upper	0.9949	0.9520	0.8822	0.7741	0.6224	0.5554	0.4987	0.3967
	Lower	0.9949	0.9517	0.8798	0.7653	0.5929	0.5190	0.4418	0.3049
GCIM		0.9949	0.9518	0.8805	0.7674	0.6026	0.5312	0.4612	0.3371
MCS		0.9949	0.9520	0.8820	0.7731	0.6179	0.5476	0.4871	0.3748
GCIM error		0.0000	0.0002	0.0015	0.0057	0.0153	0.0164	0.0259	0.0377

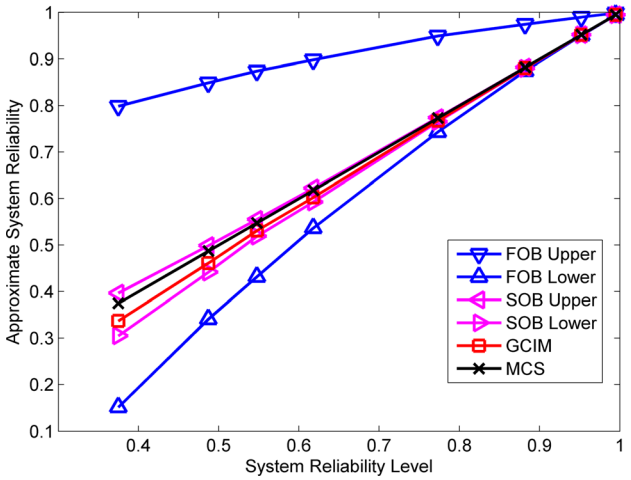

Fig. 4 Results of system reliability analysis at eight different reliability levels

levels (e.g., greater than 0.95), which are often encountered in engineering practices, than those at low system reliability levels.

This case study considers the first- and second-order CI events. The CIM produces numerical error because of the ignorance of the probabilities of the third- or higher-order CI events. The effects of the third- or higher-order CI events tend to increase as the system reliability decreases, simply because the probabilities of joint events (joint failure events or CI events) are usually bigger at low reliability level than at high reliability level. This is also true for the reliability bound methods. As can be observed from Table 3 and Fig. 4, the lower the system reliability, the larger the CIM estimation error and the wider the bounds produced by FOB and SOB. Thus for series systems, the CIM produces smaller numerical error at a high system reliability level than that at a lower level. This is valid only for series systems. When only probabilities of the first- and the second-order joint events are used for system reliability analysis, the GCIM will provide comparable results with the average of SOBs. However, compared with SOBs, the GCIM not only provides system reliability analysis formula with probabilities of any order joint events, but also provide a way of evaluating the probabilities of high order joint events as a function of the probabilities of CI events and probabilities of high order joint events as shown in Eq. (1).

4.2 Example 2. A Ten Brittle Bar Parallel System. The following ten-bar system example is used to demonstrate the effectiveness of the GCIM framework for parallel systems. As shown in Fig. 5, ten brittle bars are connected in parallel to sustain a load applied at one end. This case study is modified from the example employed in Ref. [25]. Ten bars are all brittle with different

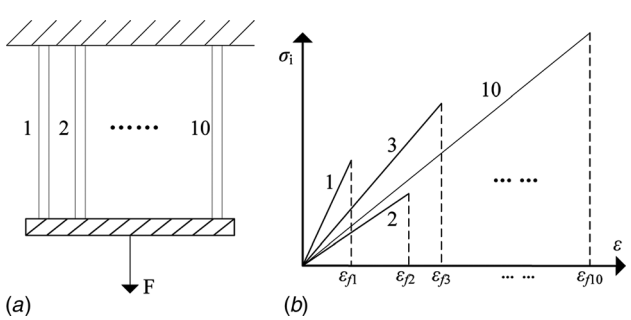

Fig. 5 Ten brittle bar parallel system: (*a*) system structure model; (*b*) brittle material behavior in a parallel system

fracture strain limits ε_{fi}, $1 \le i \le 10$, which are sorted in an ascending order. If the exerted strain ε is between the $(i-1)$th and ith fracture strain limits, i.e., $\varepsilon_{f(i-1)} \le \varepsilon < \varepsilon_{fi}$, bar components with fracture strains below ε_{fi} will fail, and the allowable load is then the sum of the strength of components with fracture strains equal to or above ε_{fi}. Therefore, the strain level corresponding to the overall maximum allowable load is among the ten fracture strain limits. As the overall maximum allowable load, the system strength R_T can be formulated in the following:

$$R_T = \max_{\varepsilon}\left\{\sum_{j=1}^{10} R_j(\varepsilon)\right\} = \max_{1\le i\le 10}\left\{\sum_{j=i}^{10} R_j(\varepsilon_{fi})\right\} = \max\left\{\sum_{j=1}^{10} R_j(\varepsilon_{f1}), \sum_{j=2}^{10} R_j(\varepsilon_{f2}), \ldots, R_{10}(\varepsilon_{f10})\right\} \quad (20)$$

For example, if the exerted strain ε is equal to the fracture strain ε_{f2}, the first brittle bar fails due to the fracture and no longer contributes to the overall system strength. Thus, the system strength R_T at this fracture strain is the sum of strength of the other nine brittle bars. The brittle bar system fails to sustain the load F only if the system strength at any of the ten fracture strains is smaller than the load F. This is a parallel system with ten components, corresponding to the ten fracture strains. The component safety events can be expressed in terms of several random variables,

$$G_i = F - \sum_{j=i}^{10} R_j(\varepsilon_{fi}) = F - \sum_{j=i}^{10} (E_j A_j)\cdot \varepsilon_{fi}, \quad 1 \le i \le 10 \quad (21)$$

where R_j represents the allowable load that can be sustained by the jth brittle bar, A_j the cross-section area of the jth brittle bar, and E_j the Young's modulus of the jth brittle bar.

Random variables and their random properties are summarized in Table 4. Ten different system reliability levels are used for comparison with ten different loading conditions (F). These loading points are used to validate the GCIM method at different reliability levels. Table 5 summarizes the results of system reliability analyses which are illustrated in Fig. 6. It can be seen that the first-order bounds are too wide to be of practical use, whereas the second-order bounds method gives tighter system reliability

Table 4 Statistical information of input random variables for the ten bar system

Random variable	Mean	Standard deviation	Distribution type
E_1–E_{10} (GPa)	200.0	10.0	Gumbel
A_1 (mm^2)	100.0	5.0	Lognormal
A_2 (mm^2)	120.0	5.0	Lognormal
A_3 (mm^2)	140.0	5.0	Lognormal
A_4 (mm^2)	140.0	10.0	Lognormal
A_5 (mm^2)	140.0	10.0	Lognormal
A_6 (mm^2)	150.0	10.0	Lognormal
A_7 (mm^2)	150.0	15.0	Lognormal
A_8 (mm^2)	150.0	15.0	Lognormal
A_9 (mm^2)	200.0	15.0	Lognormal
A_{10} (mm^2)	300.0	25.0	Lognormal
ε_{f1}	0.0010	0.0002	Uniform
ε_{f2}	0.0012	0.0003	Uniform
ε_{f3}	0.0018	0.0004	Uniform
ε_{f4}	0.0025	0.0005	Uniform
ε_{f5}	0.0027	0.0006	Uniform
ε_{f6}	0.0030	0.0007	Uniform
ε_{f7}	0.0033	0.0008	Uniform
ε_{f8}	0.0036	0.0009	Uniform
ε_{f9}	0.0040	0.0010	Uniform
ε_{f10}	0.0050	0.0011	Uniform
F (kN)	—	30.0	Normal

Table 5 Results of system reliability analysis with MCS, FOB using MCS, SOB using MCS, and GCIM using MCS ($N = 1 \times 10^6$)

Analysis method		System reliability level at each design									
		1	2	3	4	5	6	7	8	9	10
FOB	Upper	0.4133	0.5639	0.7331	0.9216	1.0000	1.0000	1.0000	1.0000	1.0000	1.0000
	Lower	0.1594	0.2054	0.2507	0.2974	0.3444	0.4395	0.4865	0.5334	0.5803	0.9705
SOB	Upper	0.3537	0.467	0.5854	0.7065	0.8293	1.0000	1.0000	1.0000	1.0000	1.0000
	Lower	0.3192	0.4062	0.4849	0.5507	0.6068	0.6917	0.7161	0.7459	0.7897	0.9943
GCIM		0.3417	0.4456	0.5490	0.6482	0.7388	0.8714	0.9017	0.9069	0.9051	0.9943
MCS		0.3301	0.4272	0.5226	0.6131	0.6961	0.8314	0.8813	0.9192	0.9476	0.9998
GCIM error		0.0116	0.0184	0.0264	0.0351	0.0427	0.0400	0.0204	0.0123	0.0425	0.0055

bounds compared with the first-order bounds method. It is expected based on the results that the GCIM method can produce accurate system reliability estimates at a wide variety of reliability levels and that this high accuracy can be maintained at high reliability levels, which are often encountered in engineering practices. Similar to the first case study, only the first- and second-order CI events were considered and the error for the GCIM comes from the effects of the third- or higher-order CI events. However, for a parallel system these effects tend to decrease as the system reliability decreases; thus the error at a low system reliability level is smaller than that at a higher system reliability level, as observed from Fig. 6.

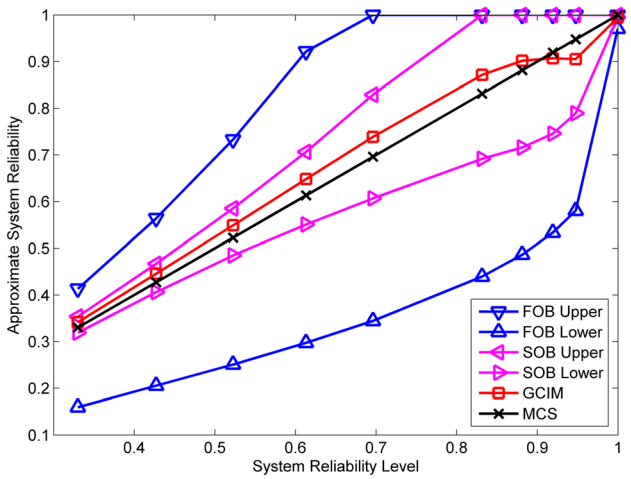

Fig. 6 Results of system reliability analysis at ten different reliability levels

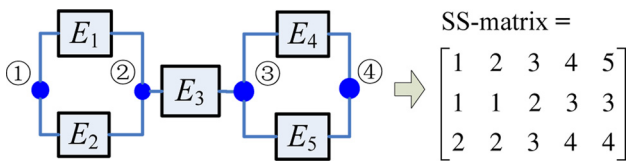

Fig. 7 System block diagram and SS-matrix for example 3

4.3 Example 3. A Mathematical Mixed System Example. This mathematical example is used to demonstrate the application of the generalized CIM for system reliability analysis of a mixed system. Two random variables X_1 and X_2, which follow normal distributions with standard deviation of 0.5, are considered in this example. Five component safety events, E_1 to E_5, are defined as

$$E_1 = \{1 - X_1^2 X_2/15 \le 0\}$$
$$E_2 = \left\{1 - (X_1 + X_2 - 5)^2/30 - (X_1 - X_2 - 12)^2/50 \le 0\right\}$$
$$E_3 = \{1 - 45/(X_1^2 + 8X_2 + 5) \le 0\}$$
$$E_4 = \left\{20\Big/\left[(X_1 - X_2 + 1)^2 + 5X_2 + 1\right] - 1 \le 0\right\}$$
$$E_5 = \{4\cos(\pi X_1/6)\sin(\pi X_2/8) - 1 \le 0\} \quad (22)$$

The above-presented component safety events constitute a mixed system with the corresponding reliability block diagram and SS-matrix shown in Fig. 7. The BDD diagram can then be derived as shown in Fig. 8, which indicates the following mutually exclusive system path sets as

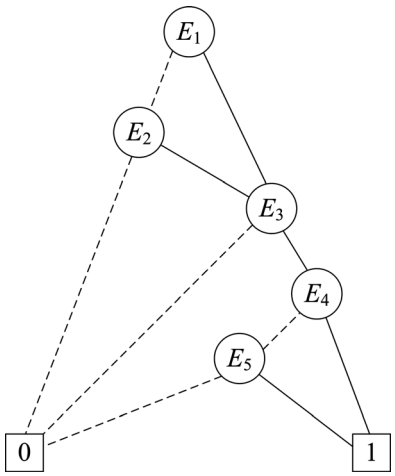

Fig. 8 BDD diagram for example 3

Table 6 Results of different system reliability analysis methods: GCIM and MCS ($N = 1 \times 10^6$)

Analysis method	System reliability at each point									
	1	2	3	4	5	6	7	8	9	10
X_1	2.5151	2.0847	5.0506	4.7959	4.6556	3.0842	1.5647	4.2499	3.2640	3.4877
X_2	4.3171	3.5262	1.6407	1.7620	1.7078	2.6952	0.0159	0.5421	1.0281	0.7726
GCIM	0.3579	0.4619	0.5760	0.6710	0.7676	0.8598	0.9319	0.9625	0.9951	0.9987
MCS	0.3548	0.4607	0.5750	0.6708	0.7675	0.8598	0.9319	0.9625	0.9951	0.9987
GCIM error	0.0031	0.0012	0.0010	0.0001	0.0000	0.0000	0.0000	0.0000	0.0000	0.0000

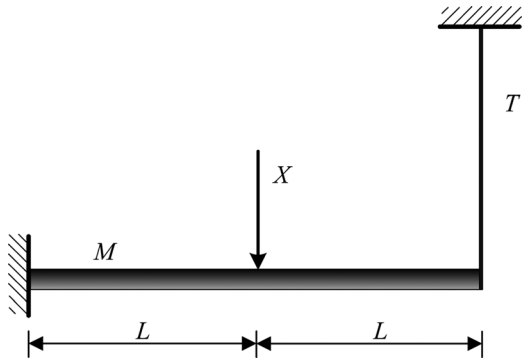

Fig. 9 A cantilever beam-bar system

Table 7 Statistical information of input random variables

Random variable	Mean	Standard deviation	Distribution type
L	5.0	0.05	Normal
T	1000	300	Normal
M	150	30	Normal
X	u_x	20	Normal

$$\text{Path set} = \{E_1E_3E_4,\ \bar{E}_1E_2E_3E_4,\ E_1E_3\bar{E}_4E_5,\ \bar{E}_1E_2E_3\bar{E}_4E_5\}$$

System reliability analysis is carried out using the GCIM and MCS at ten different sets of mean values of X_1 and X_2 as shown in Table 6. These inputs lead to ten different system reliability levels. The comparison in Table 6 suggests that the GCIM provides fairly accurate results for the mixed system problem. The small difference is due to the errors in the CIM approximations to the path sets that are mainly introduced by ignorance of the probabilities of third- and higher-order joint failure events.

4.4 Example 4. A Cantilever Beam-Bar Mixed System. The following cantilever beam-bar system [15] is employed in this study to demonstrate the effectiveness of the GCIM framework for mixed system reliability analysis. The system is considered as an ideally elastic-plastic cantilever beam supported by an ideally rigid-brittle bar, with a load applied at the midpoint of the beam, as shown in Fig. 9. There are three failure modes and five independent failure events $\bar{E}_1-\bar{E}_5$. These three failure modes are formed by different combinations of failure events.

- First failure mode—the fracture of the brittle bar (event $\bar{E}_1$) occurs, and subsequently the formation of a hinge at the fixed point of the beam (event $\bar{E}_2$).
- Second failure mode—the formation of a hinge at the fixed point of the beam (event $\bar{E}_3$) followed by the formation of another hinge at the midpoint of the beam (event $\bar{E}_4$).
- Third failure mode—the formation of a hinge at the fixed point of the beam (event $\bar{E}_3$) followed by the fracture of the brittle bar (event $\bar{E}_5$).

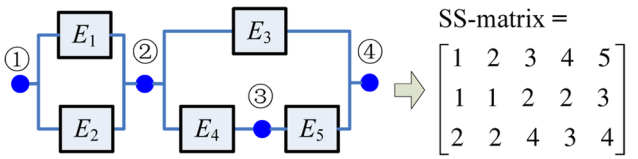

Fig. 10 System block diagram and SS-matrix for the cantilever beam-bar example

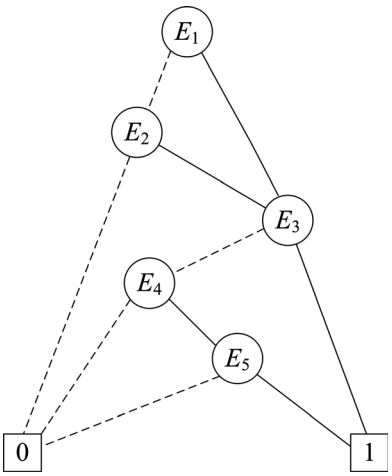

Fig. 11 BDD diagram for the cantilever beam-bar example

The five safety events can be expressed as

$$\begin{aligned} E_1 &= \{X,T|5X/16 - T \le 0\} \\ E_2 &= \{X,L,M|LX - M \le 0\} \\ E_3 &= \{X,L,M|3LX/8 - M \le 0\} \\ E_4 &= \{X,L,M|LX/3 - M \le 0\} \\ E_5 &= \{X,L,M,T|LX - M - 2LT \le 0\} \end{aligned} \tag{23}$$

Considering these three failure modes, the system success event can be obtained as

$$E_S = (E_1 \cup E_2) \cap \{E_3 \cup (E_4 \cap E_5)\} \tag{24}$$

The statistical information of the random input variables is given in Table 7. Ten different system reliability levels are used for comparison with ten different loading conditions (X).

The reliability block diagram along with the SS-matrix is shown in Fig. 10. Based on this SS-matrix, the BDD diagram can be constructed as shown in Fig. 11.

The BDD indicates the following mutually exclusive system path sets as

$$\text{Path set} = \{E_1E_3,\ \ \bar{E}_1E_2E_3,\ \ E_1\bar{E}_3E_4E_5,\ \ \bar{E}_1E_2\bar{E}_3E_4E_5\}$$

The system reliability analysis is carried out using the GCIM with ten different loading conditions (ten different u_x values for the X)

Table 8 Results of different system reliability analysis methods: GCIM and MCS ($N = 1 \times 10^6$)

	System reliability at each point									
Analysis method	1	2	3	4	5	6	7	8	9	10
u_x	100	90	85	80	70	60	50	40	20	10
GCIM	0.3546	0.4981	0.5724	0.6444	0.7708	0.8666	0.9308	0.9681	0.9954	0.9995
MCS	0.3548	0.4982	0.5725	0.6445	0.7708	0.8667	0.9309	0.9681	0.9954	0.9995
GCIM error	0.0002	0.0001	0.0001	0.0001	0.0000	0.0001	0.0001	0.0000	0.0000	0.0000

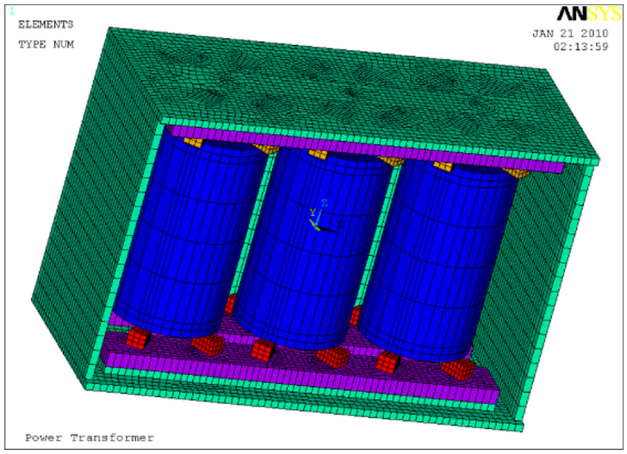

Fig. 12 A power transformer finite element model (without covering wall)

as shown in Table 8. The MCS is used for a benchmark solution and the results are also summarized in Table 8. We expect based on the results that the GCIM can give accurate system reliability estimates for mixed systems at various reliability levels.

4.5 Example 5. A Power Transformer Joint Mixed System Problem. Power transformers are among the most expensive elements of high-voltage power systems [26]. The power transformer vibration induced by the magnetic field loading will cause the windings support joint loosening or the fatigue failures, which will gradually increase the vibration amplitude of the winding and eventually damage the core [27]. In this case study the proposed GCIM has been applied for the system reliability analysis of the power transformer winding support joints. We considered four failure modes, which are the fatigue failures at the four winding support joints. A power transformer simulation model was built using the finite element analysis tool ANSYS 10 (see Fig. 12). Figure 13 shows the details of the winding bolt joint, which assembles the windings of the power transformer with the bottom fixture. The transformer is fixed at the bottom and the vibration load is applied to the magnetic core with the frequency of 120 Hz. This case study employed ten random variables, as listed in Table 9, which include the geometric tolerances and material properties.

This winding support system with the four joints was treated as a 3-out-of-4 system as shown in Fig. 14, which means that the system becomes safe only if at least three out of the four support joints survive. The CI-matrix for this case study was evaluated using the MCS (with 1000 samples), as shown in Fig. 15. Figure 16 shows the system reliability block diagram and Table 10 displays the SS-matrix for this transformer joint system.

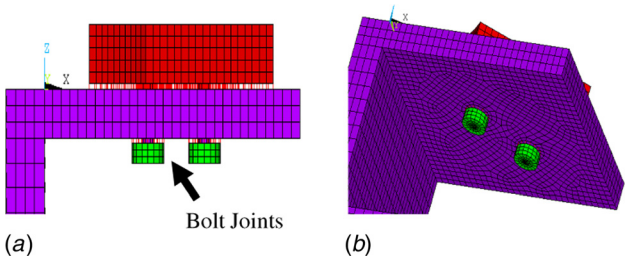

Fig. 13 Winding support bolt joint: (*a*) side view, (*b*) bottom view

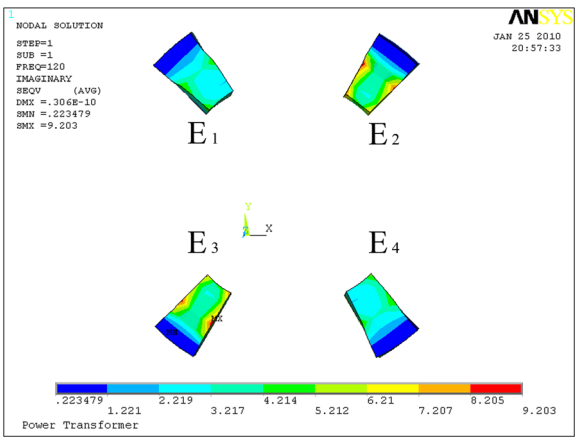

Fig. 14 3-out-of-4 system with support joints

$$\text{CI}-\text{matrix} = \begin{bmatrix} 0.999 & 0.000 & 0.238 & 0.242 \\ - & 0.999 & 0.238 & 0.242 \\ - & - & 0.761 & 0.008 \\ - & - & - & 0.757 \end{bmatrix}$$

Fig. 15 CI-matrix for the power transformer example

The mutually exclusive path sets can be determined using the BBD (see Fig. 17) as

$$\text{Path set} = \{E_1E_2E_3,\ \ \bar{E}_1E_2E_3E_4,\ \ E_1\bar{E}_2E_3E_4,\ \ E_1E_2\bar{E}_3E_4\}$$

These path sets are mutually exclusive with the series system structure, as discussed in Sec. 3.3. As shown in Table 11, the

Table 9 Random property of input variables for the power transformer example

Random variable	Physical meaning	Mean	Standard deviation	Distribution type
X_1	Wall thickness	3	0.06	Normal
X_2	Angular width of support joints	15	0.3	Normal
X_3	Height of support joints	6	0.12	Normal
X_4	Young's modulus of support joint	2×10^{12}	4×10^{10}	Normal
X_5	Young's modulus of loosening joints	2×10^{10}	4×10^{8}	Normal
X_6	Young's modulus of winding	1.28×10^{12}	3×10^{10}	Normal
X_7	Poisson ratio of joints	0.27	0.0054	Normal
X_8	Poisson ratio of winding	0.34	0.0068	Normal
X_9	Density of joints	7.85	0.157	Normal
X_{10}	Density of windings	8.96	0.179	Normal

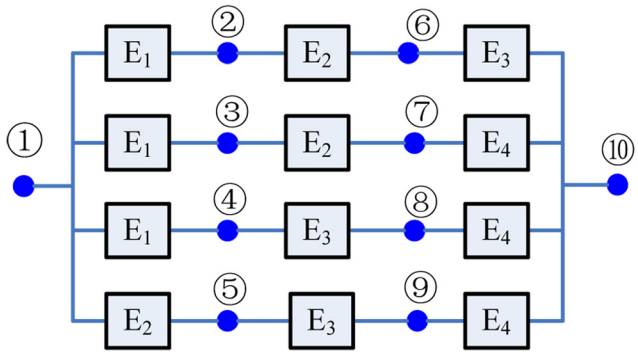

Fig. 16 System reliability block diagram for the power transformer example

Table 10 System Structure matrix for the power transformer case study

Component No.	1	1	1	2	2	2	3	3	3	4	4
Starting node	1	1	1	1	2	3	4	5	6	7	8
End node	2	3	4	5	6	7	8	9	10	10	10

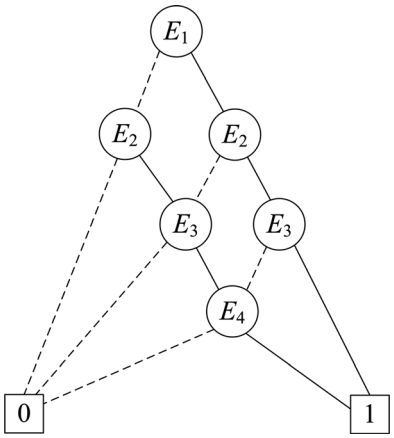

Fig. 17 BDD diagram for the power transformer example

reliabilities for these mutually exclusive path sets can be obtained and the system reliability for this transformer joint system can be estimated using Eq. (17). Based on the results, the GCIM is expected to accurately assess system reliabilities of large-scale engineered systems. This case study demonstrates the feasibility and capability of the GCIM for system reliability analysis with any system structure.

5 Conclusion

This paper presents the Generalized Complementary Intersection Method (GCIM) for system reliability analysis. The GCIM generalizes the original CIM so that it can be used for system reliability analysis regardless of system structures (series, parallel, and mixed system). This generalization leverages two ideas: (i) transforming a parallel system to the equivalent series system using De Morgan's law to derive a closed-form system reliability formula; (ii) defining a new System Structure matrix (SS-matrix) and employing the Binary Decision Diagram (BDD) technique to develop a unified system reliability analysis framework for mixed systems. This unified framework automatically decomposes a mixed system (represented by a system block diagram) into multiple disjoint series systems (not independent but mutually exclusive), which allows one to apply the original CIM to these series systems and obtain a unique estimate of system reliability, and that is precisely the main contribution of our paper, brought by way of a BDD-based algorithm for computing mutually exclusive path sets. Indeed, the basic idea behind this generalization is to add another computational layer in the original CIM structure and to reformulate the problem in a way that allows for the use of the original CIM. Such a reformulation is an extension of our original work, with the advantage that it greatly expands the application domain and achieves a unique solution of system reliability regardless of system structures (series, parallel, and mixed systems). The five case studies (with one for series system, one for parallel system, and three for mixed system) were used to demonstrate that the proposed GCIM can assess system reliability accurately regardless of the system structures. It was compared with the first- and second-order bound methods and the MCS in the first two case studies (series and parallel systems) and, subsequently, the MCS only in the last three case studies (mixed systems). As observed through the case studies, the GCIM offers the generic system reliability analysis framework and thus shows a great potential to enhance our capability and understanding of system reliability analysis.

Acknowledgment

The work presented in this paper has been partially supported by US National Science Foundation (NSF) under Grant No. GOALI-07294, U.S. Army TARDEC by the STAS contract (TCN-05122), General Motors under Grant No. TCS02723, and by the SNU-IAMD.

Nomenclature

E_i = safe event (or first-order complementary intersection event) of ith system component
E_{ij} = complementary intersection event for ith and jth system components
E_iE_j = joint event of ith and jth system components
P_f = probability of failure
Φ = standard Gaussian cumulative distribution function
$P(E_i)$ = probability of event E_i
$f_x(x)$ = probability density function
p_{fs} = probability of system failure
G_i = function of the ith constraint
b = reliability index

Table 11 Results of GCIM for power transformer case study comparing with MCS (10,000 samples)

	Reliability of path set (series system)				
Analysis method	$E_1E_2E_3$	$\bar{E}_1E_2E_3E_4$	$E_1\bar{E}_2E_3E_4$	$E_1E_2\bar{E}_3E_4$	System reliability
GCIM	0.761	0.000	0.000	0.002	0.763
MCS	**0.7611**	**0.0018**	**0.0000**	**0.0000**	**0.7629**

Appendix A

Appendix A provides a brief overview of the BDD technique, including the fundamentals and implementation details.

A.1 Fundamentals of BDD. A BDD was first introduced by Lee [22], and further studied by Akers [23] and Randal [28], who contributed to make this technique widely known. More recently, it has been widely used to solve a fault tree model for reliability analysis [29–32]. The Binary Decision Diagram (BDD) is a directed acyclic graph which consists of logic paths starting from a root vertex and terminating at a state 1 vertex (system success) or a state 0 vertex (system failure). Derived based on Shannon decomposition [33], the BDD encodes the success and failure logics of a system by decomposing it into a number of mutually exclusive path and cut sets.

In Figs. 1 and 2, an example system block diagram represented by a system structure matrix (SS-matrix) is converted to a BDD which encodes the reliability logic of this system. As can be seen, the BDD is basically a special rooted tree, composed of two types of vertices: (i) a terminal vertex has an attribute value 0 or 1 corresponding to the final state of the system; and (ii) a nonterminal vertex has an attribute corresponding to a component safety event in the system block diagram. Each path is traced along the left child branch (component fails) marked by a dashed line and right child branch (component succeeds) marked by a solid line. The ordering of all vertices in an ordered BDD ensures that different variables appear in the same order on all paths from the root vertex. In Fig. 1, the ordering of vertices reads $E_1 < E_2 < E_3 < E_4$. It is important to note that the ordering scheme can significantly affect the number of nodes in the BDD. Thus, it is of great importance to select an ordering scheme that minimizes the size of the BDD and hence the number of resultant path sets, particularly for large complex systems.

In general, the correspondence between a Boolean function $f(E_1,\ldots, E_m)$ representing system success and failure logics and its BDD can be defined in a recursive way as follows: (1) for terminal vertex, f takes constants 0 (system failure) and 1 (system success), respectively; (2) for nonterminal vertex E_i, f takes an if-then-else (ite) format based on Shannon decomposition, expressed as

$$f = ite(E_i,\ f_{i,0},\ f_{i,1}) = \bar{E}_i f_{i,0} + E_i f_{i,1} \tag{A1}$$

where the Boolean functions $f_{i,0}$ and $f_{i,1}$ are represented by the left and right child branches of E_i, respectively, and take the following forms:

Pseudo code: % Construct BDD and Mutually Exclusive Path Set from SSM

```
% Initialization
  Matrix{1} = SS_matrix;   Path_Set = ∅;   Index{1} = ∅;
  N_Elem: No. of elements in SS_matrix;
  N_Node: No. of nodes in SS_matrix
% Construct BDD & Find Mutually Exclusive Pathes
  For i = 1 to N_Elem
    j = 0;   New_Matrix = ∅;   New_Index = ∅
    While Matrix ≠ ∅
        If Elem_j ⊂ Matrix{1}
          If Node_1 ⊂ Matrix{1} \ Elem_j
            New_Index{++j} = Index{1} ⋃ Elem_j = 0
            New_Matrix{j} = Matrix{1} \ Elem_j
          End If
          If Endnode_Elem_j = N_Node
            Add {Index{1} ⋃ Elem_j = 1} into Path_Set
          Else
            New_Index{++j} = Index{1} ⋃ Elem_j = 1
            New_Matrix{j} = Matrix{1} \ Elem_j
            Update New_Matrix{j};
          End If
        Else  New_Index{++j} = Index{1};   New_Matrix{j} = Matrix{1}
        End if
        Matrix = Matrix \ Matrix{1}
    End While
    Matrix = New_Matrix; Index = New_Index
  End For
  Update Path_Set
% End of the Pseudo code
```

Fig. 18 Pseudocode for constructing BDD and computing mutually exclusive path set

Pseudo code: % Construct BDD and Mutually Exclusive Path Set from SSM

Initialize

$Matrix\{1\} = [1\ \ 1\ \ 2;\ \ 2\ \ 2\ \ 4;\ 3\ 2\ 3;\ 4\ 3\ 4]';$

$Path\_Set = \varnothing;\quad Index\{1\} = \varnothing;\quad N\_elem{=}4;\quad N\_node = 4$

$i = 1$: % Decomposition on Element 1

$New\_Index\{1\} = [1\quad 0]'$

$New\_Matrix\{1\} = Matrix\{1\} \setminus Elem_1$

$= [2\ \ 2\ \ 4;\ 3\ 2\ 3;\ 4\ 3\ 4]' \xrightarrow{Node\ 1\ \text{excluded, To terminal "0"}} New\_Matrix\{1\} = [];$

$New\_Index\{2\} = [1\quad 1]'$

$New\_Matrix\{2\} = [2\ \ 2\ \ 4;\ 3\ 2\ 3;\ 4\ 3\ 4]' \xrightarrow{E_1=1,\ \text{Update Node 2} \rightarrow \text{Node 1}} [2\ \ 1\ \ 4;\ 3\ 1\ 3;\ 4\ 3\ 4]'$

$i = 2$: % Decomposition on Element 2

$New\_Index\{1\} = [1\quad 1;\ 2\ \ 0]'$

$New\_Matrix\{1\} = [3\ 1\ 3;\ 4\ 3\ 4]'$

$Path\_Set\{1\} = [1\quad 1;\ 2\ \ 1]' \leftarrow$ *Element* 2 connect Node 1 and Node 4

$i = 3$: % Decomposition on Element 3

$New\_Index\{1\} = [1\quad 1;\ 2\ \ 0;\ 3\ \ 0]'$

$New\_Matrix\{1\} = [4\ 3\ 4]' \xrightarrow{Node\ 1\ \text{excluded, Go to terminal "0"}} New\_Matrix\{1\} = [];$

$New\_Index\{2\} = [1\quad 1;\ 2\ \ 0;\ 3\ \ 1]'$

$New\_Matrix\{2\} = [4\ 3\ 4]' \xrightarrow{E_3=1,\ \text{Update Node 3} \rightarrow \text{Node 1}} [4\ 1\ 4]'$

$i = 4$: % Decomposition on Element 4

$New\_Index\{1\} = [1\quad 1;\ 2\ \ 0;\ 3\ \ 1;\ 4\quad 0]'$

$New\_Matrix\{1\} = [\ \ ]' \leftarrow$ Terminal "0"

$Path\_Set\{2\} = [1\quad 1;\ 2\ \ 0;\ 3\ \ 1;\ 4\quad 1]' \quad \leftarrow$ *Element* 4 connect Node 1 and Node 4

End of the Program, Exit Path Set $\{E_1E_2,\ E_1\bar{E}_2E_3E_4\}$

Fig. 19 BBD and mutually exclusive path set example using the pseudocode

$$f_{i,0} \equiv f(E_1, \ldots, E_i = 0, \ldots, E_m)$$
$$f_{i,1} \equiv f(E_1, \ldots, E_i = 1, \ldots, E_m) \tag{A2}$$

Here, we can clearly observe two disjointed branches, which is one of the key features of a BDD.

A.2 Constructing BDD and Computing Mutually Exclusive Path Set from SS-Matrix. A path set, or a combination of component safety or failure events resulting in system success, corresponds to a BDD path that terminates at a state 1 terminal vertex. For example, the path marked with a dotted line ellipse in Fig. 2 corresponds to a path set E_1E_2. Following another BDD path terminating at a state 1 terminal vertex gives another path set $E_1\bar{E}_2E_3E_4$. Since the BDD encodes the logic function of the system success in a disjoint form, the path sets obtained from the BDD are mutually exclusively. A widely used algorithm for constructing a BDD and deriving minimal cut sets from the BDD was developed by Rauzy [29]. In this study, we have developed an algorithm for building a BDD and computing minimum path sets from a SS-matrix. The algorithm starts from the decomposition of root vertex and evolves throughout all vertexes until the terminal vertex. The pseudocode for the developed algorithm is shown in Fig. 18.

A.3 BBD and Mutually Exclusive Path Set Example Using the Pseudocode. The following example uses the system shown in Fig. 2 to demonstrate the developed algorithm for constructing the BDD and computing the mutually exclusive path set. Following the algorithm, the mutually exclusive path set for this example can be obtained with two disjoint paths, as the detailed process shown in Fig. 19. The probability of occurrence of the system success event, or system reliability R_S, can be computed as the sum of the probabilities of these mutually exclusive path sets, expressed as

$$R_s = P(\text{Path}_1 + \text{Path}_2) = P(\text{Path}_1) + P(\text{Path}_2)$$
$$= P(E_1E_2) + P(E_1\bar{E}_2E_3E_4) \tag{A3}$$

References

[1] Rahman, S., and Xu, H., 2004, "A Univariate Dimension-Reduction Method for Multi-Dimensional Integration in Stochastic Mechanics," Probab. Eng. Mech., **19**(4), pp. 393–408.

[2] Huang, B., and Du, X., 2006, "Uncertainty Analysis by Dimension Reduction Integration and Saddlepoint Approximations," ASME J. Mech. Des., **128**(1), pp. 26–33.

[3] Youn, B. D., Xi, Z., and Wang, P., 2008, "Eigenvector Dimension Reduction (EDR) Method for Sensitivity-Free Uncertainty Quantification," Struct. Multidiscip. Opt., **37**(1), pp. 13–28.

[4] Xiong, F., Greene, S., Chen, W., Xiong, Y., and Yang, S., 2010, "A New Sparse Grid Based Method for Uncertainty Propagation," Struct. Multidiscip. Opt., **41**(3), pp. 335–349.

[5] Du, X., and Chen, W., 2004, "Sequential Optimization and Reliability Assessment Method for Efficient Probabilistic Design," ASME J. Mech. Des., **126**(2), pp. 225–233.

[6] Youn, B. D., Choi, K. K., and Du, L., 2005, "Enriched Performance Measure Approach (PMA+) for Reliability- Based Design Optimization," AIAA J., **43**(4), pp. 874–884.

[7] Youn, B. D., Choi, K. K., and Yi, K., 2005, "Performance Moment Integration (PMI) Method for Quality Assessment in Reliability-Based Robust Design Optimization," Mech. Based Des. Struct. Mach., **33**, pp. 185–213.
[8] McDonald, M., and Mahadevan, S., 2008, "Reliability-Based Optimization With Discrete and Continuous Decision and Random Variables," ASME J. Mech. Des., **130**(6), 061401.
[9] Kim, C., and Choi K. K., 2008, "Reliability-Based Design Optimization Using Response Surface Method With Prediction Interval Estimation," ASME J. Mech. Des., **130**(12), 121401.
[10] Ditlevsen, O., and Bjerager, P., 1984, "Narrow Reliability Bounds for Structural Systems," J. Eng. Mech., **110**(5), pp. 671–693.
[11] Thoft-Christensen, P., and Murotsu, Y., 1986, *Application of Structural Reliability Theory*, Springer, Berlin.
[12] Karamchandani, A., 1987, "Structural System Reliability Analysis Methods," John A. Blume Earthquake Engineering Center, Stanford University, Stanford, CA, Report No. 83.
[13] Xiao, Q., and Mahadevan, S., 1998, "Second–Order Upper Bounds on Probability of Intersection of Failure Events," J. Eng. Mech., **120**(3), pp. 49–57.
[14] Ramachandran, K., 2004, "System Reliability Bounds: A New Look with Improvements," Civ. Eng. Environ. Syst., **21**(4), pp. 265–278.
[15] Song, J., and Der Kiureghian, A., 2003, "Bounds on Systems Reliability by Linear Programming," J. Eng. Mech., **129**(6), pp. 627–636.
[16] Nguyen, T. H., Song, J., and Paulino, G. H., 2010, "Single-Loop System Reliability-Based Design Optimization Using Matrix-Based System Reliability Method: Theory and Applications," ASME J. Mech. Des., **132**(1), 011005.
[17] Mahadevan, S., and Raghothamachar, P., 2000, "Adaptive Simulation for System Reliability Analysis of Large Structures," Comput. Struct., **77**(6), pp. 725–734.
[18] Zou, T., and Mahadevan, S., 2006, "Versatile Formulation for Multi-Objective Reliability-Based Design Optimization," ASME J. Mech. Des., **128**(6), pp. 1217–1226.
[19] Zhou, L., Penmetsa, R. C., and Grandhi, R.V., 2000, "Structural System Reliability Prediction Using Multi-Point Approximations for Design," 8th ASCE Specialty Conference on Probabilistic Mechanics and Structural Reliability, PMC2000-082.
[20] Youn, B. D., and Wang, P., 2009, "Complementary Intersection Method for System Reliability Analysis," ASME J. Mech. Des., **131**(4), 041004.
[21] Ditlevsen, O., and Bjerager, P., 1984, "Narrow Reliability Bounds for Structural Systems," J. Eng. Mech., **110**(5), pp. 671–693.
[22] Lee, C. Y., 1959, "Representation of Switching Circuits by Binary-Decision Programs," Bell Syst.Tech. J., **38**, pp. 985–999.
[23] Akers, B., 1978, "Binary Decision Diagrams," IEEE Trans. Comput., **27**(6), pp. 509–516.
[24] Liang, J. H., Mourelatos, Z. P., and Nikolaidis, E., 2007, "A Single-Loop Approach for System Reliability-Based Design Optimization," ASME J. Mech. Des., **126**(2), pp. 1215–1224.
[25] Mahadevan, S., Zhang, R. X., and Smith, N., 2001, "Bayesian Networks for System Reliability Reassessment," Struct. Safety, **23**(3), pp. 231–251.
[26] Rivera, H. L., Garcia-Souto, J. A., and Sanz, J., 2000, "Measurement of Mechanical Vibrations at Magnetic Cores of Power Transformers with Fiber-Optic Interferometric Intrinsic Sensor," IEEE J. Sel. Top. Quantum Electron., **6**(5), pp. 788–797.
[27] Kim, Y.-D., Shim, J.-M., Park, W.-Y., Kim, S.-J., Hyun, D.-S., and Lee, D.-D., 2009, "Structure Vibration Analysis of a Power Transformer (154kV/60MVA/Single Phase)," Int. J. Electr. Power Energy Syst. Eng., **3**(6), pp. 330–334..
[28] Randal, E. B., 1986, "Graph-Based Algorithms for Boolean Function Manipulation," IEEE Trans. Comput., **35**(8), pp. 677–691.
[29] Rauzy, A., 1993, "New Algorithms for Fault Trees Analysis," Reliab. Eng. Syst.Saf., **40**(3), pp. 203–211.
[30] Zang, X., Sun, H., and Trivedi, K. S., 1999, "A BDD-Based Algorithm for Reliability Analysis of Phased-Mission Systems," IEEE Trans. Reliab., **48**(1), pp. 50–60.
[31] Tang, Z., and Dugan, J. B., 2006, "BDD-Based Reliability Analysis of Phased Mission Systems with Multimode Failures," IEEE Trans. Reliab., **55**(2), pp. 350–360.
[32] Prescott, D. R., Remenyte-Prescott, R., Reed, S., Andrews, J. D., and Downes, C.G., 2009, "A Reliability Analysis Method Using BDDs in Phased Mission Planning," Proc. Inst. Mech. Eng. Part O: J. Risk Reliab., **223**, pp. 133–143.
[33] Shannon, C. E., 1938, "A Symbolic Analysis of Relay and Switching Circuits," Trans.AIEE, **57**(6), pp. 713–723.